Analog/RF Solutions Enabling Compact Full-Duplex Radios

Björn Debaillie, *Member, IEEE*, Dirk-Jan van den Broek, *Student Member, IEEE*, Cristina Lavín,
Barend van Liempd, *Member, IEEE*, Eric A. M. Klumperink, *Senior Member, IEEE*, Carmen Palacios,
Jan Craninckx, *Fellow, IEEE*, Bram Nauta, *Fellow, IEEE*, and Aarno Pärssinen, *Senior Member, IEEE*

Abstract—In-band full-duplex sets challenging requirements for wireless communication radios, in particular their capability to prevent receiver sensitivity degradation due to self-interference (transmit signals leaking into its own receiver). Previously published self-interference rejection designs require bulky components and/or antenna structures. This paper addresses this form-factor issue. First, compact radio transceiver feasibility bottlenecks are identified analytically, and tradeoff equations in function of link budget parameters are presented. These derivations indicate that the main bottlenecks can be resolved by increasing the isolation in analog/RF. Therefore, two design ideas are proposed, which provide attractive analog/RF-isolation and allow integration in compact radios. The first design proposal targets compact radio devices, such as small-cell base stations and tablet computers, and combines a dual-port polarized antenna with a self-tunable cancellation circuit. The second design proposal targets even more compact radio devices such as smartphones and sensor network nodes. This design builds on a tunable electrical balance isolator/duplexer in combination with a single-port miniature antenna. The electrical balance circuit can be implemented for scaled CMOS technology, facilitating low cost and dense integration.

Index Terms—In-band full-duplex, self-interference isolation, dual polarized antenna, tunable duplexer, electrical balance, transceiver macro-modeling.

I. INTRODUCTION

TODAYS evolution in wireless communication is characterized by a tremendous growth and dynamism in data traffic and user access [1], [2]. To sustain this evolution, improved air interface techniques are required to increase the spectral efficiency. The exploitation of in-band full-duplex (FD) in wireless communications targets to improve this efficiency
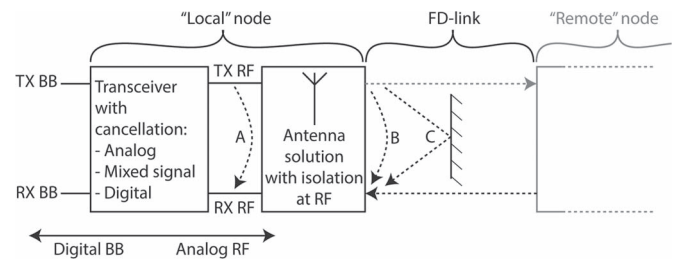
Fig. 1. FD-link between a "Local" and "Remote" radio node. Self-interference enters the receiver through various paths: direct crosstalk (A), limited antenna isolation (B) and reflections through the environment (C).

by using the same resources to transmit and receive, i.e., simultaneous transmission and reception at the same carrier frequency.

Different attractive network concepts have been developed [3]–[6] which exploit FD capabilities in wireless communication radios to improve the capacity and user access. Especially in cellular, access point and mesh networks, FD has the potential to mitigate some fundamental problems like hidden terminals, bandwidth degradation and network latency [7]–[9].

The benefits at network level however rely on the availability of full-duplex radios. The key challenges in full-duplex radios are:

— *Isolation*: to *prevent* the RF-signal generated by the local transmitter (TX) from leaking onto its own receiver (RX), where it causes self-interference.

— *Cancellation*: to *subtract* any remaining self-interference from the RX path using knowledge of the TX signal.

As the receiver is capturing a signal coming from a distant source, the self-interference is much stronger in power in the absence of isolation/cancellation. As it occupies the same frequency band, it interferes with the reception and may hinder the receiver sensitivity and therefore the link throughput. The TX signal in a typical link is in excess of 100 dB above its RX noise floor, requiring isolation and cancellation to provide roughly 100 dB rejection of the self-interferer if no performance compromise can be accepted. These numbers and associated hardware bottlenecks will be refined for different application scenarios in Section II.

Fig. 1 illustrates a full-duplex link between two wireless radio nodes, the 'local' and 'remote' one. Assuming a symmetrical link, the discussions that will follow apply to either radio node. Hence only the 'local' node with its downlink is fully depicted, as well as the associated self-interference via various cross-talk and reflection paths.

In the recent years, several designs have been published dealing with the self-interference problem. They propose different self-interference rejection techniques, covering isolation, cancellation, and combinations of the two.

Isolation of the receiver from self-interference is achieved by minimizing the parasitic signal propagation from the transmitter to its own receiver. Prior designs mainly focus on multiple antenna techniques, where the antenna spacing and positioning is exploited [7], [10]–[17]. These multiple antenna techniques achieve up to 40 dB of isolation, but prevent dense integration due to the required physical distances between the antennas. An alternative technique which uses one antenna for simultaneous transmission and reception, relies on a circulator to isolate the receiver from the transmitter [18], [19]. Unfortunately, circulators provide a moderate isolation between TX and RX of about 20 dB, they show nonlinear behavior and they are considered bulky and expensive for consumer equipment operating below 6 GHz.

Self-interference *cancellation* is achieved by subtracting the interference in the receiver path, where the subtracted signal is a modified copy of the transmitted signal. This modification mimics the channel path between the points where signals are sampled (transmitter) and subtracted (receiver). The effectiveness of cancellation highly depends on the accuracy with which the transmitted signal can be copied, modified and subtracted. Three main cancellation architectures are described in literature [7], [10]–[13], [20]. The first architecture, called *digital cancellation*, processes the signals completely in the digital domain, leveraging all digital benefits. However, this cannot remove self-interference in the analog receiver chain, and is thus unable to prevent the analog circuitry to block the reception due to nonlinear distortion or saturation. This architecture can provide up to 30–35 dB cancellation in practice [12], [13], limited by a noisy estimate of the self-interference channel and noisy components of the self-interferer that cannot be cancelled. A second architecture is *analog cancellation*, which uses a tap of the actual RF transmit signal for use in cancellation. This is beneficial as the cancellation signal includes all transmitter impairments, and it relaxes requirements further downstream, but it requires processing the cancellation signal in the analog RF domain. This architecture provides cancellation performance up to 60 dB [18]. The third architecture is *mixed-signal cancellation*: the digital TX signal is processed and converted to analog RF, where subtraction occurs. This requires a dedicated additional up-convertor, which in practice introduces its own noise and distortion [21] and therefore limits its cancellation to 35 dB.

To achieve an overall self-interference rejection of more than 100 dB, a *combination* of isolation and cancellation techniques implemented in digital, analog and RF is required. Literature reports up to 60 dB of total self-interference rejection when combining analog/RF isolation with digital cancellation [7], [10], [13], [14], [21]. Although few techniques indicate higher rejection [11], [12], [18], all published designs require bulky components and/or antenna structures, hampering the development of compact wireless full-duplex radios. Only few of the relevant designs have published form-factor measures as listed in Table I.

TABLE I
FORM FACTOR MEASURES PRESENTED IN LITERATURE

Form factor	Covered in form factor	Reference
Laptop size 330x230 mm	Antenna spacing for TX and RX antenna	[5]
Laptop screen size	Antenna spacing for 2xTX and RX antennas	[12]
100x100 mm	Analog cancellation board (excl. antenna, circulator etc.)	[18]
70x80 mm	Integrated 2xTX and RX antennas	[14]

TABLE II
FORM FACTOR OF WIRELESS COMMUNICATION DEVICES

BASE STATIONS	Femto-cell	236 x 160 x 76 mm
	Pico-cell	426 x 336 x 128 mm
	Macro-cell	1430 x 570 x 550 mm
ACCESS POINTS/ USER EQUIPMENT	Netbook	285 x 202 x 27.4 mm
	Tablet PC	241 x 186 x 8.8 mm
	Smartphone	124 x 59 x 7.6 mm
M2M	Sensor nodes	50 x 50 x 50 mm

Our work aims to solve this form-factor issue by focusing on solutions that can be integrated in the compact radio device as a separate module, or integrated on the radio chip (system on chip (SoC)). Such integration would permit the design of commercially attractive compact full-duplex radios for different applications. To further motivate this aim, consider the annual growth of the amount of mobile broadband subscribers of about 40% [2]. These subscribers are increasingly diverse covering user terminals and self-operating machines. Compact radio devices will be dominantly employed, estimated to 27.4% smart phones and 16.5% M2M communication devices by 2017 compared to all portable devices [1]. This evolution towards portable devices with smaller form factor is especially challenging for full-duplex communication devices, because the existing self-interference rejection solutions mainly rely on physical dimensions (i.e., antenna spacing) and bulky components hampering dense integration. This paper focuses on analog/RF self-interference rejection solutions that can be densely integrated in compact radio devices. Table II gives realistic radio form factor indications over different applications. To preserve the form factor of these radios, the dimension of the analog/RF self-interference rejection solution should typically not **exceed** 10% of the sizes listed in Table II. In this work both compact radios (femto-cell base-stations, netbooks and tablet PC's) and extremely compact radios (smartphones and sensor nodes) are considered. Please note that size and cost really matters in commercial applications, and compromises in performance may be required to make FD radio commercially viable.

In order to optimize performance, cost and size, it is crucial to explore different design options and their trade-offs. Hence, this paper first analyzes the self-interference mechanisms and effects, and identifies the feasibility bottlenecks for a compact radio. It systematically analyzes a set of transceiver requirements needed for integrated transceiver design and circuit simulation. To the best of our knowledge, such a systematic analysis has not been published before for full duplex. Based on sets of

specifications for low-end to high-end application scenarios, different transceiver bottlenecks are identified and quantified. It is shown how requirement bottlenecks can be relaxed or resolved by increasing RF-isolation. Then two designs that improve isolation while achieving a small factor are proposed. The first design targets applications such as small-cell base stations and notebooks, whereas the second design targets more compact devices, such as smartphones and sensor nodes. The first solution combines passive cancellation based on a dual-port polarized antenna with self-tunable RF cancellation. The second solution is a single-port antenna circuit which uses electrical balance directly at the antenna interface to isolate TX and RX signals. By virtue of its tunability, robust and frequency agile isolation may be achieved. Both presented techniques are compatible with other cancellation techniques, which are required to further increase the overall self-interference rejection performance.

The next section will systematically derive a set of full-duplex transceiver requirements considering various transceiver impairments. It also aims to find a set of feasible building block specifications for a compact full-duplex radio. Sections III and IV describes the two analog/RF self-interference techniques, where Section III focuses on the dual-port directional antenna solution and Section IV focuses on the electrical balance technique. Finally, Section V summarizes the main conclusions.

II. TRANSCEIVER REQUIREMENTS AND BOTTLENECKS

A. Transceiver Impairments

Fig. 1 illustrated a full-duplex wireless link between two radio nodes, suffering from self-interference. In practice, this self-interference consists of multiple components as the transmit signal is corrupted by different impairments, such as non-linearity, phase- and quantization noise [18]. Some of these by-products are noisy, others are deterministic. This transmit signal, including its by-products, is coupled into the receiver through various paths indicated in Fig. 1, e.g., direct crosstalk (A), TX-RX antenna leakage due to limited isolation (B), and reflections on nearby objects in the environment (C). To achieve a receiver sensitivity similar to conventional half-duplex radios is very challenging, as all self-interference components should be suppressed to below the receiver noise floor. This likely requires isolation in the antenna solution combined with cancellation in the transceiver.

Fig. 2 shows the key "local node" signals limiting the FD link budget when receiving a remote transmitter signal, assuming both nodes operate at equal average transmit power. The locally transmitted signal (Local TX) consists of a clean signal and its by-products due to transmitter impairments (half-circle). Isolation at RF (e.g., antenna isolation) will attenuate the self-inferences coupled to the receiver (Local RX), along with its transmitter impairments. Additional by-products will arise on this large signal due to receiver impairments (circle). Cancellation techniques are required to further reduce the self-interference and its by-products towards the receiver digital baseband (Local BB), ideally to below the noise floor.

It is well known from literature that high isolation is desired for FD-radios and some promising results have been achieved.
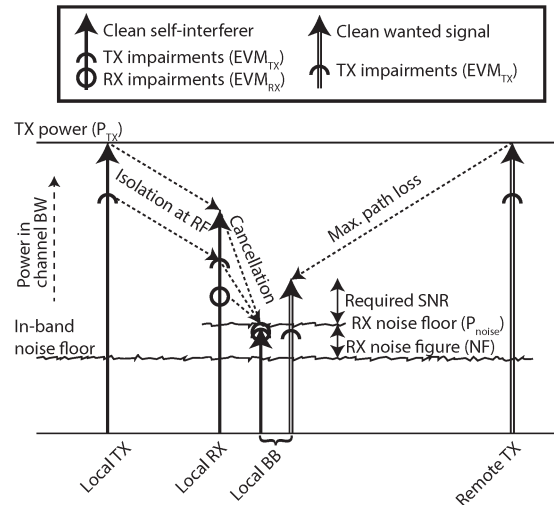

Fig. 2. Relation between various in-band power levels in a full-duplex link budget. The combination of isolation and cancellation techniques suppress all self-interference components, preferably to below the receiver noise floor.

What has not been explored much are the consequences of limited robustly achievable isolation, e.g., if compact low cost radios have to work under varying environmental conditions. The question then arises how transceiver requirements change as a function of the RF-isolation and link budget parameters, and whether a viable user scenario is still feasible. Table I shows some results of an analysis that will be detailed below. It analyzes several important transceiver requirements (bold fonts) as a function of several assumption (italics). Comparing the outcomes to typically feasible transceiver specifications taken from [22] as shown in the right side column, bottlenecks are identified and marked. These bottlenecks can be resolved by increasing the amount of RF-isolation or by improvements in transceiver design. In the following, the equations needed for transceiver design are derived.

Starting from the link budget parameters bandwidth (BW), transmission power (P_{TX}) and receiver noise figure (NF), the in-band receiver noise floor (P_{noise}) is calculated as:

$$P_{\mathrm{noise}} \text{ [dBm]} = -174 \frac{\mathrm{dBm}}{\mathrm{Hz}} + 10^* \log\left(\mathrm{BW} \text{ [Hz]}\right) + \mathrm{NF} \text{ [dB]}. \tag{1}$$

In Table III, typical numbers for a low-end, mid-end and high-end wireless link scenario are given, where the high-end specifications correspond to a commercial 54-Mbps WLAN link with 64-QAM OFDM [22]. The mid- and low-end scenarios have significantly relaxed transmit power and noise figure and a factor 2 lower bandwidth, which is deemed still viable for some shorter range links, e.g., for sensor networks.

Table III lists the outcome of (1) and also the resulting difference between the transmit power and the noise floor, indicating that 79 to 116 dB of isolation/cancellation is required to prevent sensitivity losses compared to a half-duplex link. In practical antenna solutions [7], [17], the effective isolation is limited to approximately 40 dB, also due to reflections from the environment. Therefore, an additional cancellation of 39 to 76 dB would be required to exceed the noise floor.

If the antenna solution is pushed to achieve more isolation, the self-interference path likely becomes more dominated by

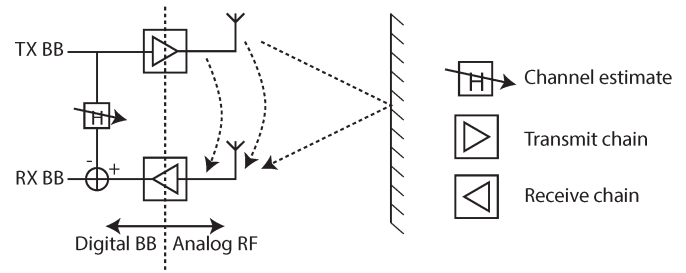| *Scenario difficulty* *RF-Isolation in dB*	*Eqn*	*Low-end* *20dB/40dB*		*Mid-end* *40dB/60dB*		*High-end* *60dB/80dB*		*feasible*
BW (MHz)		10	10	10	10	20	20	20
P_{TX} (dBm)		0	0	10	10	20	20	20
NF (dB)		25	25	15	15	5	5	5
P_{noise} (dBm)	(1)	-79	-79	-89	-89	-96	-96	-96
P_{TX}-P_{noise} (dB)		79	79	99	99	116	116	116
Isolation (dB)		20	40	40	60	60	80	
P_{SI} =P_{TX}-Isolation (dBm)		-20	-40	-30	-50	-40	-60	
EVM$_{TX}$ (dB)	(2)	**-59**	**-39**	**-59**	**-39**	**-56**	**-36**	**-40**
$P_{IM3,TX}$ (dBc)	(3)	-59	-39	-59	-39	-56	-36	-40
OIP3$_{TX}$ (dBm)	(4)	**30**	**20**	**40**	**30**	**48**	**38**	**40**
$CP_{1dBTX} \approx OIP3_{TX}$-10 (dBm)		20	10	30	20	38	28	30
OBO$_{TX}$ (dB)		**20**	**10**	**20**	**10**	**18**	**8**	**10**
DAC margin (dB)		15	15	20	20	25	25	25
DAC_DR (dB)	(7)	74	54	79	59	81	61	65
DAC bits=DAC_DR/6.02		**12**	**9**	**13**	**10**	**13**	**10**	**11**
$P_{IM3,RX}$ (dBm)	=(1)	-79	-79	-89	-89	-96	-96	
$CP_{1dBRX} \approx IIP3_{RX}$-10 (dBm)		**-20**	**-40**	**-30**	**-50**	**-40**	**-60**	**-30**
IIP3$_{RX}$ (dBm)	(5)	**10**	**-21**	**-1**	**-31**	**-12**	**-42**	**0**
ADC-margin (dB)		20	20	25	25	30	30	30
ADC_DR (dB)		79	59	84	64	86	66	70
ADC bits		**13**	**10**	**14**	**10**	**14**	**11**	**11**
PN (dBc)	(6)	**-62**	**-42**	**-62**	**-42**	**-59**	**-39**	**-40**
PN (deg)	(7)	**0.05**	0.46	**0.05**	0.46	**0.06**	0.64	0.57

Fig. 3. Self-interference suppression techniques are required to prevent the reduction of receiver sensitivity for FD e.g., isolation at the antenna(s) and cancellation in the digital baseband.

In all three full-duplex scenarios mentioned before, an isolation of 40 dB and an EVM of -25 dB would result in a self-interference due to TX impairments well above the receiver noise floor, limiting the receiver sensitivity. To solve this problem, the TX EVM requirement should be better than:

$$EVM_{TX} \text{ [dB]}$$
$$\leq -\left(P_{TX} \text{ [dBm]} - P_{noise} \text{ [dBm]} - \text{Isolation [dB]}\right). \quad (2)$$

The resulting values are shown in Table III, where each scenario is extended with an extra 20 dB of isolation to relax the EVM to a likely feasible value. Note that this EVM is no longer dictated by the modulation scheme, but by the FD constraint. Alternatively, extra analog cancellation can relax the EVM requirement by including the effects of the transmitter impairments in analog cancellation path [18].

EVM is a lumped term for errors that actually results from several causes, e.g., distortion, DAC dynamic range and phase noise. The related requirement will be modeled in the next paragraphs. Quadrature imbalance (I/Q amplitude and phase mismatch) is not modeled here as effective techniques exist to calibrate and suppress it [24].

1) Transmitter Nonlinearity: In-band EVM due to transmitter nonlinearity is often mainly due to 3rd order intermodulation distortion. For low EVM a weakly nonlinear model with a 3rd-order output referred intercept point ($OIP3_{TX}$) can be adequate [25], while the 1 dB compression point provides an estimate of the upper limit of output power range.

Without distortion, the "clean self-interferer" enters the receiver at a power level of P_{SI}. Ideally its distortion content should stay below P_{noise}. Therefore, the transmitted distortion products ($P_{IM3,TX}$) should satisfy (see also Table III)

$$P_{IM3,TX} \text{ [dBc]} \leq P_{SI} \text{ [dBm]} - P_{noise} \text{ [dBm]}. \quad (3)$$

With a transmitted power P_{TX}, the required OIP3 at the transmitter thus equals

$$OIP3_{TX} \text{ [dBm]} \geq P_{TX} \text{ [dBm]} + \frac{P_{IM3,TX} \text{ [dBc]}}{2}. \quad (4)$$

Assuming a simple weakly nonlinear memory-less transmitter model, the 1 dB compression point will be approximately 10 dB below $OIP3_{TX}$ and the output back-off (OBO_{TX}) of the transmitter can be calculated (Table III). In all scenarios, the transmitter has to be operated at a larger back-off than normally required for the corresponding link (e.g., in the high-end scenario, more than the normally required 6–8 dB for 802.11g

reflections from the environment, which can make the self-interference channel very frequency-selective [12]. Further cancellation of this frequency-selective self-interference can be addressed leveraging OFDM modulation and digital processing techniques to estimate the self-interference channel using pilot sequences and tones. Combining isolation and OFDM-based cancellation in the digital domain could theoretically form a full-duplex solution, as depicted in Fig. 3. The transmit signal is fed through a digital estimate of the self-interference channel, and subtracted from the received signal in digital baseband. However, this solution puts stringent requirements on the transmitter and receiver, which will be illustrated in the next sections.

B. Transmitter Impairments

Transmitter Error Vector Magnitude (EVM) is a commonly used metric to quantify the transmitter performance, which covers the main in-band impairments, albeit in a lumped fashion. In conventional half-duplex radios, the EVM toughest requirement results from the most complex modulation scheme to be used. E.g., for the high-end scenario, to demodulate 64-QAM OFDM for a 54-Mbps WLAN link, better than 5.6% (-25 dB) EVM is required [23].

WLAN [26]). This causes power-inefficient operation. A potential solution direction to reduce the required back-off is linearization by pre-distortion [27]. Alternatively, analog cancellation performed at RF includes the transmitter nonlinearities in the cancellation signal and therefore makes stronger distortion products acceptable [18].

2) DAC Dynamic Range: The main DAC requirement in a half-duplex transceiver is the dynamic range to transmit the most complex modulated signal with sufficient fidelity. E.g., for the high-end scenario, to transmit 64-QAM OFDM for a 54-Mbps WLAN link, about 8 bits are required in the DAC [26] resulting in about 50 dB dynamic range. Since the EVM requirement for this link is −25 dB, about 50 dB − 25 dB = 25 dB margin is taken in the DAC to make its EVM contribution (quantization noise and clipping noise due to high peak-to-average ratios) non-dominant. Table III lists typical DAC margins for this and the other scenarios.

In the full-duplex examples, more stringent EVM values are required in order to sufficiently cancel the self-interferer based on its digital representation, resulting in tougher DR requirements for the DAC. Assuming the same margins apply as in half-duplex, the resulting DAC dynamic range requirements are listed in Table III. The required resolution seems feasible [28], certainly for the "20 dB extra" RF-isolation cases.

C. Receiver Impairments

In a conventional half-duplex system, the receiver needs to capture the desired signal with sufficient fidelity to perform demodulation. In a full-duplex receiver, the self-interferer present at the receive port will usually be stronger than the desired receive signal (as illustrated in Fig. 2). Hence, any by-products of capturing the self-interferer should not mask the underlying desired signal. The expected issues are nonlinearity in the receiver and limited ADC dynamic range.

1) Receiver Nonlinearity: In the presence of a strong self-interferer, the receiver has to be sufficiently linear to prevent masking the desired signal with the receiver intermodulation products. If no analog cancellation is applied the required in-band input-referred 3rd-order intercept point (IIP3) [25] can be calculated, assuming a weak third-order nonlinearity. With a self-interferer power P_{SI} and a maximum strength of the 3rd-order distortion components $P_{IM3,RX}$, the required IIP3 equals:

$$\text{IIP3}_{RX} \text{ [dBm]} \geq P_{SI} \text{ [dBm]} + \frac{P_{SI} \text{ [dBm]} - P_{IM3,RX} \text{ [dBm]}}{2}. \tag{5}$$

In Table III we see the resulting value for different scenarios. Now, for the low- and mid-end scenarios the IIP3 requirement is tougher but feasible given recent improvements achieved in in-band linearity [29]. However, care must be taken that the receiver can achieve the required IIP3 at the power level P_{SI}, which may require reduction of the front-end gain to avoid compression. Applying extra analog cancellation at RF may be useful, provided this does not add any (random) components that cannot be suppressed further in the digital domain [20].

2) ADC Dynamic Range: In order to perform self-interference cancellation in the digital domain, the ADC dy-

namic range has to cover the strong self-interferer, without masking the underlying desired signal with its quantization noise. Therefore, the demands on the ADC are tougher than in half-duplex systems.

In a half-duplex link budget, the ADC has to capture the signal at the most complex modulation scheme under fading conditions, plus several margins for gain control, quantization noise and peak-to-average ratio. Typical values for 64-QAM are about 30 dB for SNR and another 30 dB for various margins [22], resulting in 60 dB ADC dynamic range. It is assumed here that the same margin applies to a full-duplex link.

The resulting ADC DR requirements and corresponding number of bits is listed in Table III, and can be very tough. Again, the though requirement can be relaxed by means of analog cancellation, where a cancellation signal is subtracted before the ADC. Unlike analog cancellation used to relax RX linearity requirement, this need not necessarily be done at RF.

D. System Level Impairments

Two system level impairments are relevant to full-duplex radios: the system clock phase noise, and the multi-path components in the self-interference path.

1) System Clock Phase Noise: Phase noise (PN), which is caused by the system clock generation and distribution system, degrades the SNR of the transmitted and the received signal. In case the transmitter and receiver operate on different system clocks, their PN will be uncorrelated. Then, TX and RX phase noise powers add and the combined noise limits the suppression that can be achieved by further cancellation at analog and digital baseband [20]. Assuming equal phase noise in the transmitter and receiver, the requirement of any single clock can be calculated:

$$\text{PN}_{RX} \text{ [dBc]} = \text{PN}_{TX} \text{ [dBc]} \leq \text{EVM}_{TX} \text{ [dB]} - 3 \text{ dB}. \tag{6}$$

For small values, this can be converted to degrees using:

$$\text{PN [deg]} \leq \arcsin\left(10^{\frac{\text{PN [dBc]}}{20}}\right). \tag{7}$$

Note that the integrated phase noise is calculated over the bandwidth BW here, and not phase noise density. The calculated values in Table III are clearly very tough without sufficient isolation.

Integrated full-duplex radios could however share a common clock as the transmitter and receiver operate simultaneously at the same frequency. Ideally, their phase noise is fully correlated and the cancellation is no longer limited by phase noise. However, in practice there will be some delay between transmission and reception of the self-interferer due to reflections [21]. This delay reduces the correlation between the transmitted and received self-interference signal and hence degrades cancellation. As a result the phase noise cancellation degrades especially at higher offset frequencies. The amount of cancellation depends on several factors: the bandwidth of the wireless link, the phase noise profile of the PLL that is used and the reflection characteristics of the self-interference channel. This is an important topic for further research.

2) Multi-Path Reflection: In a realistic environment, transmitted signals may be reflected back to their own receiver through different paths which are each characterized by an attenuation and a delay. When leveraging OFDM modulation, the net effect is a subcarrier-dependent attenuation and phase shift, i.e., a frequency-selective channel. Multi-path reflections of the self-interferer can be cancelled by virtue of OFDM [28], but this requires a clean (noise-free) transmit signal. Realistically, the transmitter impairments add noise and distortion by-products which are also reflected via multiple paths. Distortion by-products can be reduced in the digital domain as was recently demonstrated in [18]. Noise by-products require, however, that an exact analog copy of the transmit signal is fed through circuitry that mimics the self-interference channel including the time delays. Implementing these delays at RF may provide robust cancellation [18], but leads to a bulky solution. Basically physical delay lines are needed with equal length as the delay path they model, divided by the ratio of the propagation velocities of associated propagation media (typically $2:1$ for air compared to cables). Such a direct delay line implementation is not suitable for full CMOS integration, so alternative compact solutions are wanted.

E. Transceiver Design Trade-Offs

The formulas derived above are very useful for spreadsheet calculation to assess overall feasibility and also as starting point for deriving sub-block specification. The results in Table III indicate that even for a low-end very relaxed scenario 40 dB of RF-isolation is very much wanted. For the high-end case this increases to 60 or even 80 dB, which is extremely challenging. The tables indicates that not only phase noise but also transmitter linearity are very critical aspects, while receiver linearity becomes a bottleneck at low isolation values. Design innovations will hopefully move or remove some of the indicated bottlenecks, and the analysis above is believed to be very useful for future work on full-duplex transceiver design.

III. DUAL-POLARIZED FULL-DUPLEX ANTENNA

As shown in the previous section, isolation at the antenna is key in mitigating self-interference. Although interesting solutions are described in literature, their size prevents efficient integration in small form factor full-duplex radios.

Of the recent literature, [7], [11], [14]–[16], [30], most of the proposed systems operate with at least two antennas. Employing separated TX and RX antennas may provide better self-interference suppression, but these multi-antenna architectures translate the problem to the spatial domain, spoiling the far-field coverage or degrading the antenna radiation pattern. For example, [14] proposes a three antennas system using one RX antenna and two TX antennas with $180°$ phase shift. This phase shift causes TX signals to add destructively and cancel at the receiver. Similar concept is proposed by [7] where also three antennas are used. In that case, TX antennas are asymmetrically placed at distances d and $d + (\lambda/2)$ from the RX antenna causing a self-interference null at the receiver. However, these configurations creates also null regions of destructive interfer-
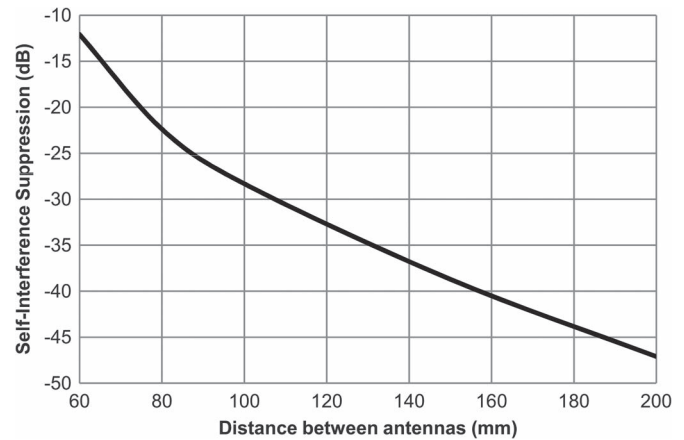

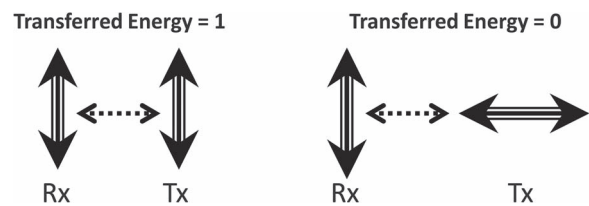Fig. 4. Self-interference suppression for antenna separation technique at 2.45 GHz.

Fig. 5. Ideal energy transfer coefficients for different polarizations.

ence in the far-field region, spoiling far-field coverage. Self-interference can also be reduced by separating the TX and RX antennas sufficiently to obtain an acceptable suppression. Fig. 4 shows the relation between the self-interference attenuation and the distance between the antennas. These results are based on full-3D electromagnetic simulations employing an omni-directional microstrip dipole at 2.45 GHz.

Based on Fig. 4, the antenna separation technique provides > 40 dB interference suppression only when antennas are separated beyond 150 mm. This large distance makes this technique unsuitable for small form-factors radio devices.

Alternatively, we propose to use only one compact antenna for both TX and RX, but still maintain the coverage area. This single antenna approach relies on polarization of the electromagnetic wave in order to reduce the self-interference between TX- and RX-waves. Ideally the transferred energy between orthogonal polarizations is zero, as illustrated in Fig. 5, and therefore the self-interference can be minimized in a full-duplex systems, provided the TX and RX signals have orthogonal polarization. For that purpose dual-polarized antennas can be used.

Dual-polarized antennas consist of single radiating elements with two ports, where in the case of full-duplex applications, one port will be connected to RX and the other port to TX. Microstrip patches are widely used as dual-polarized elements due to their low-profile, low cost and easy integration. Although common dual-polarized microstrip elements usually present poor isolation between ports (about 20–30 dB), this work introduces a microstrip stacked-patch structure with a multilayer feeding network which improves antenna cross-polarization and increases the isolation between Rx and Tx ports up to 60 dB. Fig. 6 shows the proposed antenna structure.

The proposed antenna consists of a stacked-patch structure, where the lower patch is excited from two orthogonal ports.
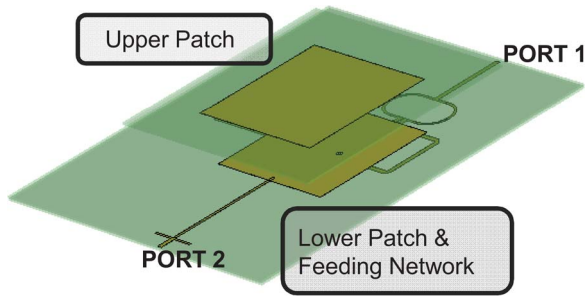
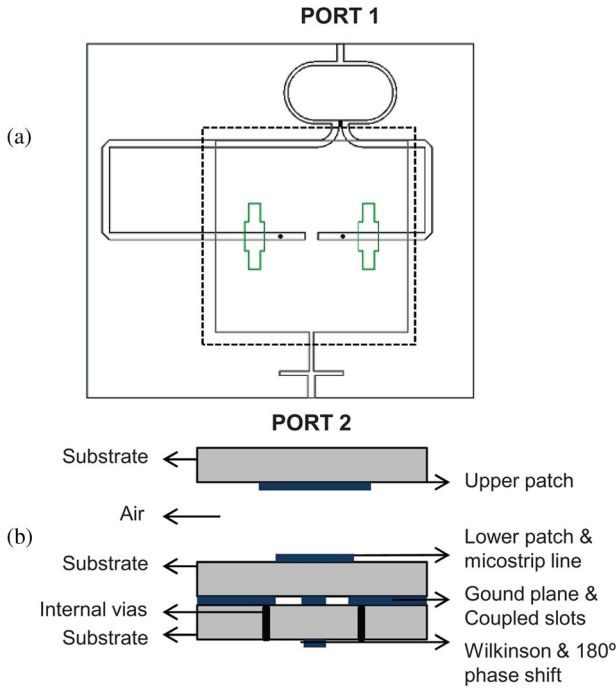Fig. 6. Dual-polarized microstrip antenna structure.

Fig. 7. Structure of the dual-polarized microstrip antenna. (a) Top view. (b) Multilayer antenna stack-up.

Both ports generate orthogonal linear polarizations by means of a slot-coupled line (Port 1—Transmission) and a standard microstrip line (Port2—Reception). Fig. 7 shows the geometry of the dual-polarized microstrip antenna as well as the antenna stack-up.

As depicted in Fig. 7, port 1 excites the patch employing coupled-slots with $180°$ phase shift introduced by a Wilkinson Divider and unequal-length microstrip lines. The slots are printed in an internal ground plane; this internal ground layer together with $180°$ phase shift excitation improves the cross-polarization purity and consequently the isolation between ports. The antenna radiation characteristics is improved by means of internal vias. Based on full-3D electromagnetic simulations of the presented design operated in free space, the antenna presents an isolation up to 60 dB between the transmitter and receiver port and 55 dB over a bandwidth of 10 MHz, as illustrated in Fig. 8. This antenna isolation exceeds the 40 dB mid-end scenario design requirement given in Table III.

The performance robustness of given antenna structure is also evaluated by simulating the effect of placing an object close to the antenna. A $60 \times 60 \times 60$ mm metallic object has
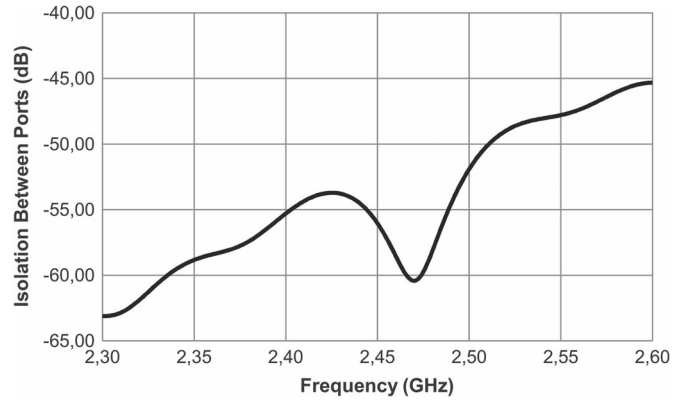

Fig. 8. Simulated isolation between the transmitter and receiver port of the dual-polarized microstrip antenna structure.
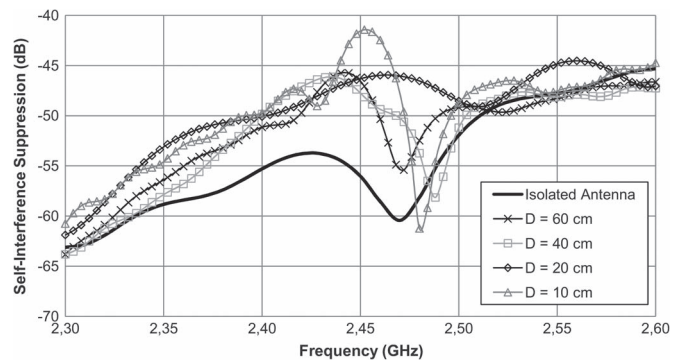

Fig. 9. Simulated antenna isolation with a near-by metallic object.

been added to the 3D electromagnetic model, and the antenna isolation is simulated for different distances between the antenna and the object. Fig. 9 shows the simulated results which indicates a limited isolation degradation, as long as the distance is 20 cm or more. Then, the degradation is limited to 8 dB (thus maintaining an antenna isolation of more than 45 dB) over a 20 MHz bandwidth at 2.45 GHz operation frequency.

Although these simulation results show a moderate impact of external elements on the isolation, reflections may, however, affect the polarization and degrade the self-interference suppression because the reflected transmission signal may have a similar polarization as the receive antenna. Therefore, it is necessary to complete the antenna isolation with a tunable cancellation stage which makes the solution more robust to environmental effects.

We propose an tunable analog cancellation, where a copy of the actual transmitted RF signal (including its in-band TX impairments) is attenuated, phase-shifted and combined with the RF received signal (before the ADC). The attenuator and phase shifter compensate the self-interference leakage due to imperfect isolation between the TX and RX. Off-the-shelf components are selected based on their linearity and distortion characteristics to avoid performance limitations as reported in [13]. Both the attenuator and the phase-shifter are tunable to cover variations in the self-interference leakage. This cancellation architecture will be self-tunable, based on the detection of the remaining self-interference in the RX path. Fig. 10, illustrates the proposed tunable cancellation block diagram in combination with the dual port antenna.
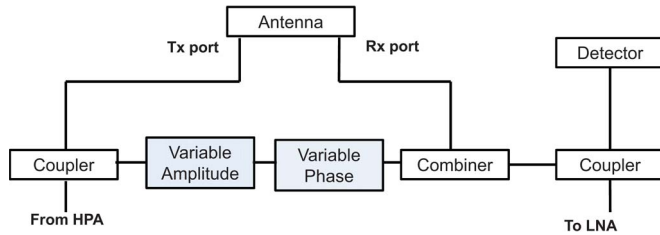
Fig. 10. Block diagram for the analog cancellation in combination with a dual-port antenna.
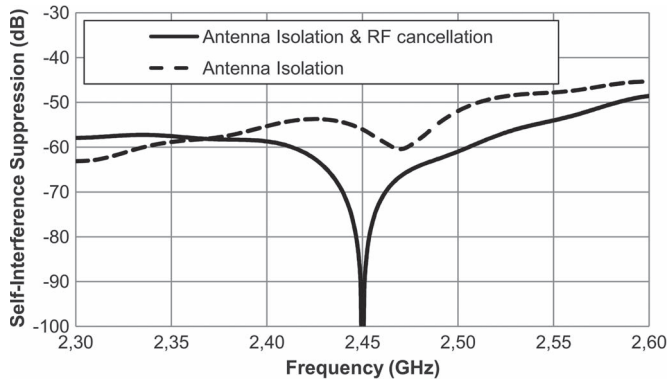

Fig. 11. Simulated isolation between the TX output and RX input port, with and without RF tunable cancellation.

The total self-interference rejection has been simulated based on a sinusoidal TX signal at 2.45 GHz by combining the antenna isolation behavior (Fig. 8) with theoretical models of an 8-bit tunable attenuator and a 10-bit tunable phase-shifter. Optimal tuning these components results in an additional RF cancellation of 21 dB over 10 MHz bandwidth, as depicted in Fig. 11. This self-interference rejection exceeds the 60 dB mid-end scenario design requirement given in Table III.

The proposed dual-polarized microstrip antenna and RF tunable cancellation circuitry combines isolation and cancellation solutions for compact radios, where the antenna dominates the size. Preliminary design indicates an antenna size of 90 × 90 mm when Rogers substrate with a dielectric constant of 3.55 is used. However, the size of the antenna could be reduced by 68–70%, by making use of substrates with higher dielectric constants and by minimizing the size of Wilkinson Divider and microstrip delay lines. Then, the antenna structure measures 30 × 30 mm, which is half the size of the smallest published form-factor solution presented in Table I.

IV. ELECTRICAL BALANCE RF ISOLATION

When an extremely small, integrated solution is required for a full-duplex communication devices, e.g., smartphone, a single-antenna solution favors other, more bulky solutions based on multiple antennas. Such single-antenna solution should however prevent TX signal leaking to the RX. This can be achieved by an isolator as shown in Fig. 12, which has a separate TX and RX port, but a shared TX/RX antenna. A standard miniature antenna is assumed in this case (no isolation by polarization).

In state-of-the-art cellular devices, SAW-based duplexers [31] provide the required isolation between transmission and
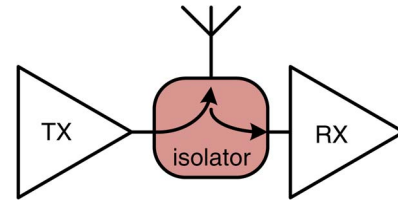

Fig. 12. Single-antenna FD solution with TX-to-RX isolation.
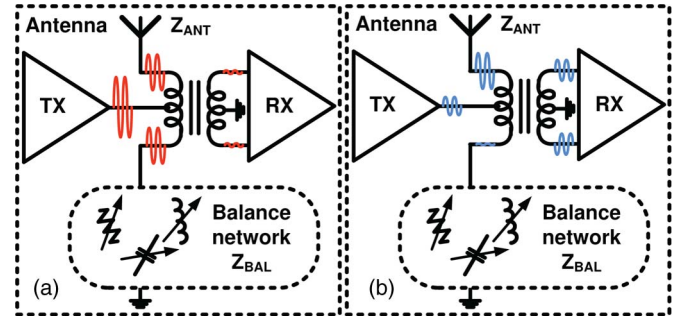

Fig. 13. Electrical balance duplexer operation principle.

reception for standards operating in Frequency Division Duplexing (FDD) mode. Furthermore, they provide out-of-band filtering to resolve many blocker issues in the path from antenna to the receiver, while reducing the spectral leakage to the adjacent channels by filtering out intermodulation products in transmission. However, such solutions are based on fixed-frequency passive filters, which only allow antenna sharing when transmission and reception operate concurrently on *different* frequencies.

Recently, the use of hybrid transformers to achieve filtering based on electrical balance has been proposed to achieve tunable duplexer filters for FDD [7], [32], [33]. In this paper, this technique is introduced in the context of full-duplex, and it is shown how it may provide self-interference isolation in RF for very compact radio devices.

A. Operating Principle

Fig. 13 shows how electrical signals transfer through a hybrid transformer, achieving electrical balance operation. Shown also are the antenna, TX, RX and a passive network called the balance network, which may consist of tunable passives, e.g., resistive, capacitive and/or inductive components.

When a signal is transmitted [Fig. 13(a)], and $Z_{ANT} = Z_{BAL}$ at the transmission frequency, the electrical signals splits up exactly between the two impedances (e.g., it is perfect common-mode to the hybrid transformer). As a result, no net differential current flows through the primary winding of the hybrid transformer, and only the common-mode leakage transfers through to the hybrid transformer secondary (i.e., RX) side, canceling any direct-path TX leakage flowing into the RX. When the first-stage low-noise amplifier in the RX chain has good common-mode rejection, the remaining common-mode is not a problem.

In reception mode [Fig. 13(b)], the antenna absorbs energy from the ether, but the same signal is not excited in the passive balance network. As a result, a differential current flows through the hybrid transformer and is transferred to the RX side.

In fact, in the ideal balance condition, the hybrid transformer is a reciprocal network [13], so that the antenna and balance network are isolated as well, like the TX and RX. For this reason, the energy absorbed by the antenna splits up between the TX and RX out- and input impedances, respectively. Near-field and far-field reflections cannot be removed by the electrical balance circuit; this requires a subsequent cancellation circuit e.g., as presented in Section III or cancellation in the digital domain.

For FD operation, both transmission and reception occur concurrently in real-time, and both principles apply. As a result, isolation is achieved from TX to RX, while transfer occurs from antenna to RX and TX to antenna, albeit with a minimal insertion loss of 3 dB due to power splitting in the hybrid transformer. This 3 dB loss however refers to an unrealistically perfect lossless implementation, where conventional FDD-systems use duplexers which also exhibits a loss of about 2.5 dB. Therefore, the additional loss of the proposed solution enabling FD operation is only 0.5 dB. Also note that a hybrid transformer can be integrated in plain silicon process technology, where a typical die-size depends on the exact implementation, but is in the order of 0.4–1 mm^2. This area is mainly determined by the hybrid transformer. This die can be mounted and interconnected with a miniature antenna (e.g., 14 mm^2 ANT-2.45-CHP from Linx Technologies) directly on the PCB of the hosting communications device. The form-factor of this design, when considering a non-size-optimized commercial off-the-shelf antenna, is at least 10 times more compact than the smallest design in Table I. The size of the electrical balance solution is sufficiently compact for integration in the smallest device listed in Table II.

B. Full-Duplex Requirements for Electrical Balance

The hybrid transformer and balance network may be co-integrated on CMOS, together with the transceiver and system-on-chip (SoC) for digital processing, to achieve a very small form-factor, mainly limited by the antenna size. There are two practical issues that complicate the implementation of this system, both relating to the antenna.

First, a practical antenna may have a widely varying impedance across frequency, but also shift when near-field objects impact the radiation pattern and thus the antenna impedance. The balance network should have sufficient tuning range to cover the impedance shift the antenna may experience. The design of the balance network is based on all realistically potential impedance shifts, while considering also the complete interconnection path towards the antenna.

Second, due to real-time variations in the antenna impedance, a fast enough (milli-second time delay) tracking algorithm must be implemented to guarantee the isolation characteristics at a given frequency. The proposed design supports such adaptation speed; it implements a 300 MHz network-on-chip [34] and the response time of the balance network is a few nano-seconds only. When used in conjunction with digital cancellation, the leakage path through the duplexer must be re-estimated in the digital algorithm at the same rate in order to maintain signal integrity in the digital domain.
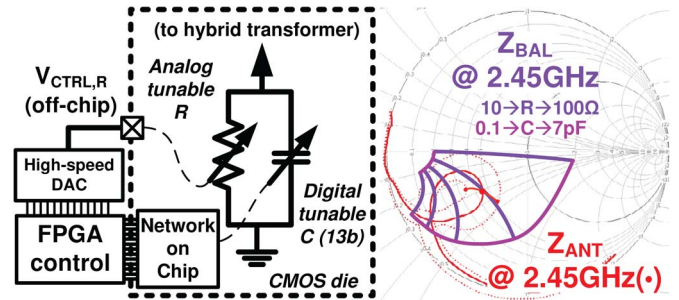

Fig. 14. (left) The R-C balance network and control; (right) measured antenna+interconnect (and variation); and theoretical balance impedance.
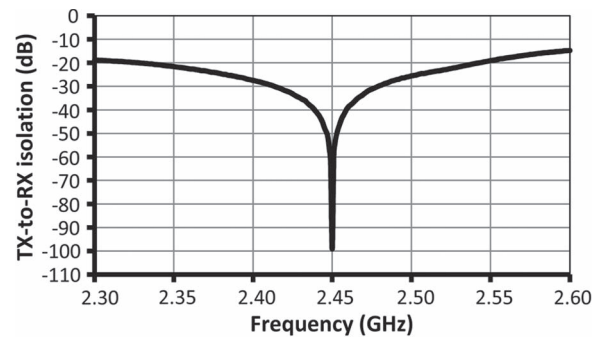

Fig. 15. Simulated RF isolation with measured antenna impedance.

As derived in Section II, an isolation of at least 50 dB across the signal bandwidth must be achieved in order to meet the total self-interference cancellation budget. For this reason, the resolution of the balance network is critical [33], and co-design with the antenna and its interconnection length is required to allow sufficient isolation bandwidth.

C. Building Block Specifications

To evaluate the required tuning range of the balance network, impedance measurements of a WiFi-specified Planar Inverted-F Antenna and interconnect to a test-chip (including bonding wire) have been made. Fig. 14 (right) shows the observed impedance variations of the antenna, including maximum observed variations in various environmental conditions.

Fig. 14 (left) shows the proposed CMOS integrated balance network that is able to operate in conjunction with this antenna. Using just a resistor and capacitor bank means no positive (inductive) imaginary impedance is covered, but thanks to the parasitic phase shifting action of the interconnect, even the Planar Inverted-F Antenna, which is mainly inductive in nature, offers a negative (capacitive) imaginary impedance at the antenna port of the hybrid transformer.

A resistor range of 10 Ω–100 Ω and a capacitor range of 800 fF–2500 fF cover the reference impedance including variations as measured from the antenna and interconnect. Those are implemented by a capacitor bank with 13-bits effective resolution and an analog-tuned resistor [32] with more than 13-bits resolution.

When an initial electrical balance condition is found by tuning the balance network to mimic the antenna impedance, Fig. 15 shows about 50 dB of isolation is achieved at 2.45 GHz over a signal bandwidth of 6 MHz and 44 dB over 10 MHz.

This RF-isolation meets the 40 dB mid-end scenario design requirement given in Table III.

V. Conclusion

This work addresses an important issue of previously published self-interference rejection designs: they generally require bulky components and/or antenna structures, which hampers the realization of compact full-duplex radios. This paper identifies feasibility bottlenecks of a compact full-duplex radios and proposes two analog/RF designs to resolve the main bottleneck.

Full-duplex sets challenging design requirements on the wireless communication transceiver, especially in comparison with half-duplex radios. Crucial transceiver requirements have been analyzed in terms of link budget parameters and the achievable RF isolation. Calculation for three scenarios in Table III indicate that, even for a low-end very relaxed scenario, 40 dB of RF-isolation is required. For the high-end case, this increases to 60 dB or even 80 dB, which is extremely challenging. Key feasibility bottlenecks are the phase noise and transmitter linearity, while receiver linearity becomes a bottleneck at low self-interference isolation values. These though design requirements can be majorly relaxed by improving isolation and cancellation at analog/RF. Therefore, two analog/RF design ideas are proposed, allowing integration in compact radio devices.

The first analog/RF design idea combines isolation and tunable cancellation by means of a dual-port polarized antenna and a self-tunable cancellation circuit, offering up to 75 dB simulated isolation (55 dB isolation +20 dB cancellation) over a bandwidth of 10 MHz at 2.45 GHz. The polarized antenna is to be implemented as microstrips on a conventional printed circuit board, which allows dense integration in a tablet computer, notebook or a small-cell base-station. A preliminary implementation indicates an antenna size of 90 × 90 mm, but is expected to scale down to 30 × 30 mm when using a higher dielectric-constant substrate.

The second analog/RF design idea exploits a tunable electrical balance isolator in combination with a single-port antenna. Implementing this in low-cost plain CMOS technology (excluding the antenna) would measure less than 1 mm^2. Given its tunability and single-port antenna connection, conventional miniature antennas are compatible with this solution. This enables integration in very compact radio devices such as smartphones and sensor network radios. Simulations indicate a 50 dB of isolation at 2.45 GHz over a signal bandwidth of 6 MHz.

Both presented techniques are compatible with digital cancellation techniques, which are required to further increase the overall self-interference rejection performance. As future work, both design ideas are implemented, and their performance will be evaluated based on measurements with and without digital cancellation.

References

[1] Cisco, Cisco Report Cisco Visual Networking Index: Global Mobile Data Traffic Forecast Update, 2012–2017, San Jose, CA, USA 2013, Cisco Report.

[2] "Measuring the Information Society: 2012," Geneva, Switzerland, ITU Rep., 2012.

[3] D. Bliss, P. Parker, and A. Margetts, "Simultaneous transmission and reception for improved wireless network performance," in *Proc. IEEE Workshop Statist. Signal*, 2007, pp. 478–482.

[4] X. Fang, D. Yang, and G. Xue, "Distributed algorithms for multipath routing in full-duplex wireless networks," in *Proc. IEEE Int. Conf. Mobile Adhoc Sensor Syst.*, 2011, pp. 102–111.

[5] A. Sahai, G. Patel, and A. Sabharwal, "Asynchronous full-duplex wireless," in *Proc. Int. Conf. Commun. Syst. Netw.*, 2012, pp. 1–9.

[6] P. C. Weeraddana, M. Codreanu, M. Latva-aho, and A. Ephremides, "The benefits from simultaneous transmission and reception in wireless networks," in *Proc. IEEE Inf. Theory Workshop*, 2010, pp. 1–5.

[7] J. I. Choi, M. Jain, K. Srinivasan, P. Levis, and S. Katti, "Achieving single channel, full duplex wireless communication," in *Proc. Int. Conf. Mobile Comput. Netw.*, 2010, pp. 1–12.

[8] A. Goldsmith, *Wireless Communications*. Cambridge, U.K.: Cambridge Univ. Press, 2005.

[9] P. C. Weeraddana, M. Codreanu, M. Latva-aho, and E. Anthony, "On the effect of self-interference cancelation in multihop wireless networks," *J. Wireless Commun. Netw.*, vol. 2010, pp. 1–10, 2010.

[10] S. Chen, M. Beach, and J. McGeehan, "Division-free duplex for wireless applications," *IEEE Electron. Lett.*, vol. 34, no. 2, pp. 147–148, Jan. 1998.

[11] M. Duarte, "Full-Duplex Wireless: Design, Implementation and Characterization," Ph.D. dissertation, Rice Univ., Houston, TX, USA, 2012.

[12] M. Duarte *et al.*, "Design and characterization of a full-duplex multiantenna system for WiFi networks," *IEEE Trans. Veh. Technol.*, vol. 63, no. 3, pp. 1160–1177, Mar. 2014.

[13] M. Jain *et al.*, "Practical, real-time, full duplex wireless," in *Proc. Int. Conf. Mobile Comput. Netw.*, 2011, pp. 301–312.

[14] A. K. Khandani, "Two-way (true full-duplex) wireless," in *Proc. Can. Workshop Inf. Theory*, 2013, pp. 33–38.

[15] A. K. Khandani, "Methods for spatial multiplexing of wireless two-way channels," U.S. Patent 7 817 641 B1, Oct. 19, 2010.

[16] M. A. Khojastepour, K. Sundaresan, S. Rangarajan, X. Zhang, and S. Barghi, "The case for antenna cancellation for scalable full-duplex wireless communications," in *Proc. Workshop Hot Topics Netw.*, 2011, pp. 1–6.

[17] D. Korpi, M. Valkama, T. Riihonen, and R. Wichman, "Implementation challenges in full-duplex radio transceivers," in *Proc. Finnish URSI Conv. Radio Sci.*, 2013, pp. 181–184.

[18] D. Bharadia, E. McMilin, and S. Katti, "Full duplex radios," in *Proc. ACM Special Interest Group Data Commun.*, 2013, pp. 1–12.

[19] Y. K. Chan, V. C. Koo, B.-K. Chung, and H.-T. Chuah, "A cancellation network for full-duplex front end circuit," *Progr. Electromagn. Res. Lett.*, vol. 7, pp. 139–148, 2009.

[20] A. Sahai, G. Patel, C. Dick, and A. Sabharwal, "On the impact of phase noise on active cancellation in wireless full-duplex," *IEEE Trans. Veh. Technol.*, vol. 62, no. 9, pp. 4494–4510, Nov. 2013.

[21] A. Sahai, G. Patel, C. Dick, and A. Sabharwal, "Understanding the impact of phase noise on active cancellation in wireless full-duplex," in *Proc. Asilomar Conf. Signals, Syst. Comput.*, 2012, pp. 29–33.

[22] I. Vassiliou, "Wireless transceiver system design for modern communication standards—Tutorial," in *Proc. IEEE Int. Solid-State Circuits Conf. Dig. Tech. Papers*, 2013, p. 499.

[23] *Part 11: Wireless LAN Medium Access Control (MAC) and Physical Layer (PHY) Specifications*, IEEE Std. 802.11-1999, 1999, p. 91.

[24] B. Debaillie, P. Van Wesemael, G. Vandersteen, and J. Craninckx, "Calibration of direct-conversion transceivers," *IEEE J. Sel. Topics Signal Process.*, vol. 3, no. 3, pp. 488–498, Jun. 2009.

[25] B. Razavi, *RF Microelectronics*. Englewood Cliffs, NJ, USA: Prentice Hall, 1997.

[26] B. Come *et al.*, "Impact of front-end non-idealities on bit error rate performance of WLAN-OFDM transceivers," in *Proc. IEEE Radio Wireless Conf.*, 2000, pp. 91–94.

[27] S. Bensmida *et al.*, "Power amplifier memory-less pre-distortion for 3GPP LTE application," in *Proc. Eur. Microw. Conf.*, 2009, pp. 1433–1436.

[28] J.-H. Tsai, Y.-J. Chen, Y.-F. Lai, M.-H. Shen, and P.-C. Huang, "A 14-bit 200 MS/s current-steering DAC achieving over 82 dB SFDR with digitally-assisted calibration and dynamic matching techniques," in *Proc. Int. Symp. VLSI Design, Autom. Test*, 2012, pp. 1–4.

[29] D. H. Mahrof, E. A. Klumperink, M. S. Oude Alink, and B. Nauta, "A receiver with in-band IIP3 > 20 dBm, exploiting cancelling of OpAmp finite-gain-induced distortion via negative conductance," in *Proc. IEEE Radio Freq. Integr. Circuits Symp.*, 2013, pp. 85–88.

[30] K. Haneda, E. Kahra, S. Wyne, C. Icheln, and P. Vainikainen, "Measurement of loop-back interference channels for outdoor-to-indoor

full-duplex radio relays," in *Proc. Eur. Conf. Antennas Propag.*, 2010, pp. 1–5.

[31] M. Hikita, N. Shibagaki, K. Sakiyama, H. Sunayama, and K. Tachibatake, "Investigation of SAW W-CDMA antenna duplexer and GSM-based FEM including duplexer," in *Proc. IEEE Ultrason. Symp.*, 2004, pp. 970–973.

[32] S. H. Abdelhalem, P. S. Gudem, and L. E. Larson, "Hybrid transformer-based tunable differential duplexer in a 90-nm CMOS process," *IEEE Trans. Microw. Theory Tech.*, vol. 61, no. 3, pp. 1316–1326, Mar. 2013.

[33] H. Darabi, A. Mirzaei, and M. Mikhemar, "Highly integrated and tunable RF front ends for reconfigurable multiband transceivers: A tutorial," *IEEE Trans. Circuits Syst. I*, vol. 58, no. 9, pp. 2038–2050, Sep. 2011.

[34] W. Eberle, "System with distributed analogue resources," U.S. Patent 8 355 408 B2, Jan. 15, 2013.

Barend van Liempd (S'08–M'11) received the B.Sc. and M.Sc. degrees in electrical engineering from the Technische Universiteit Eindhoven, Eindhoven, The Netherlands, in 2009 and 2011, respectively. His M.Sc. thesis project was on ultra-low power body area network receivers and was performed in the Holst Centre/IMEC Netherlands in Eindhoven.

In 2011, he joined the Circuits and Systems Group, IMEC, Leuven, Belgium, where his research interests include analog, mixed-signal, and RF circuit design for multi-standard radio applications in nanoscale CMOS technologies. Currently, he is working on frequency flexible duplexers that enable a highly integrated front-end module.

Björn Debaillie (M'06) received the master's degree in industrial management from the Katholieke Universiteit Leuven, Leuven, Belgium, and the B.Sc. and M.Sc. degrees in information and communication technologies from the Katholieke Hogeschool Brugge-Oostende, Ostend, Belgium.

Currently, he is a Senior Researcher with the Green Radio Program, IMEC, Leuven, Belgium, and he is a Project Manager in several national and international funded projects in the field of Green and Sustainable ICT. He has authored and co-authored 40 international journal and conference papers in various domains, and he holds several patents.

Eric A. M. Klumperink (M'98–SM'06) received the Ph.D. degree in 1997 from Twente University, Enschede, The Netherlands, where he is currently an Associate Professor in analog and RF IC electronics.

He holds several patents, and he authored and co-authored about 180 international refereed journal and conference papers. His research focus includes cognitive radio, software defined radio, and beamforming.

Dr. Klumperink serves as an Associate Editor for the *Journal of Solid-State Circuits*, and he is a Technical Program Committee Member for the ISSCC and RFIC. He is a co-recipient of the ISSCC 2002 and the ISSCC 2009 "Van Vessem Outstanding Paper Award".

Dirk-Jan van den Broek (S'14) received the B.Sc. and M.Sc. degrees in electrical engineering from the University of Twente, Enschede, The Netherlands, in 2010 and 2012, respectively. He performed both his internship and master's thesis assignment in collaboration with NXP Semiconductors, investigating a sigma delta and a time-based A/D converter concept, respectively. He is currently working toward the Ph.D. degree with the IC-Design Group, University of Twente, investigating CMOS transceiver challenges and opportunities relevant to full-duplex wireless communication.

Carmen Palacios received the B.Sc. and M.Sc. degrees in telecommunications from the Universidad de Cantabria, Santander, Spain, in 1996 and 1999, respectively.

She participated in ESA's Planck Project designing hybrid LNA at 30 GHz at the Universidad de Cantabria. In Distromel (Binéfar, Huesca), she was involved in the development of passive transceivers and traceability systems for waste management. In 2007, she joined the RF-Department, Information and Communication Technologies (TTI), Santander, Spain, working on design, assembly, integration, and measurement of equipment. She has participated in the Befemto European Project, and she is a co-author of several papers.

Cristina Lavín received the M.Sc. degree in telecommunication engineering from the University of Cantabria, Santander, Spain, in 2005.

Currently, she is with Information and Communication Technologies (TTI), Santander, Spain, where her main activities are focused on antenna design. She has been involved in several projects related to active antennas, taking part in activities of design, implementation, and calibration of antenna arrays. She has participated in different national and European funded projects. She has co-authored several conference papers and project deliverables within the framework of various research fields.

Jan Craninckx (M'98–SM'07–F'14) received the M.S. and Ph.D. degrees in microelectronics from the Katholieke Universiteit Leuven, Leuven, Belgium, in 1992 and 1997, respectively. His Ph.D. work was on the design of low-phase noise CMOS integrated VCOs and synthesizers.

From 1997 to 2002, he was a Senior RF Engineer with Alcatel Microelectronics, working on the integration of RF transceivers for GSM, DECT, Bluetooth, and WLAN. In 2002, he joined IMEC (Leuven), where he currently is the Senior Principal Scientist of the Analog Wireless Research Group. His research focuses on the design of RF transceiver front-ends for software defined radio (SDR) systems, covering all aspects of RF, analog, and data converter design.

Bram Nauta (M'91–SM'03–F'08) received the M.Sc. and Ph.D. degrees from the University of Twente, Enschede, The Netherlands, in 1987 and 1991, respectively.

In 1991, he joined the Mixed-Signal Circuits and Systems Department, Philips Research, Eindhoven, The Netherlands. In 1998, he returned to the University of Twente, as a Full Professor heading the IC Design Group. He served as an Associate Editor for IEEE TRANSACTIONS ON CIRCUITS AND SYSTEMS II (1997–1999). He was a Guest Editor, an Associate Editor (2001–2006), and later the Editor-in-Chief (2007–2010) of IEEE JOURNAL OF SOLID-STATE CIRCUITS. He was a member of the Technical Program Committee of the International Solid State Circuits Conference (ISSCC), where he served in several roles, including the European Regional Chair and the ISSCC 2013 Program Chair. He is a member of the Steering Committee and the Program Committee of the ESSCIRC conference, and he also served in the Technical Program Committee of the Symposium on VLSI Circuits. He is a co-recipient of the ISSCC 2002 and 2009 "Van Vessem Outstanding Paper Award" and several other best paper awards. He was a Distinguished Lecturer of the IEEE, he is a member of the IEEE-SSCS AdCom.

Aarno Pärssinen (S'95–M'01–SM'11) received the M.Sc., Licentiate in Technology, and Doctor of Science degrees from the Helsinki University of Technology, Espoo, Finland, in 1995, 1997, and 2000, respectively, all in electrical engineering.

In 1996, he was a Research Visitor at the University of California at Santa Barbara. From 2000 to 2011, he was with Nokia Research Center, Helsinki, Finland. During 2009–2011, he served as a member of Nokia CEO Technology Council. From 2011 to 2013, he was with Renesas Mobile Corporation, Helsinki, working as a Distinguished Researcher and RF Research Manager. In 2013, as part of business acquisition, he joined Broadcom, Helsinki, where he is currently an Associate Technical Director. His research interests include wireless systems and transceiver architectures for wireless communications, with special emphasis on the RF and analog integrated circuit and system design. He has authored and co-authored one book, one chapter of a book, and more than 50 international journal and conference papers, and he is the holder of several patents. He has served as a member of the Technical Program Committee of Int. Solid-State Circuits Conference since 2007, and he is currently the Chair of the Wireless Subcommittee.